


## Article

# Urban Particulate Matter Hazard Mapping and Monitoring Site Selection in Nablus, Palestine

Tawfiq Saleh<sup>1</sup> and Abdelhaleem Khader<sup>2,\*</sup> 

<sup>1</sup> Faculty of Graduate Studies, An-Najah National University, Nablus P4110257, Palestine; s11952750@stu.najah.edu

<sup>2</sup> Department of Civil Engineering, An-Najah National University, Nablus P4110257, Palestine

\* Correspondence: a.khader@najah.edu; Tel.: +970-59-7237419

**Abstract:** Few air pollution studies have been applied in the State of Palestine and all showed an increase in particulate matter concentrations above WHO guidelines. However, there is no clear methodology for selecting monitoring locations. In this study, a methodology based on GIS and locally calibrated low-cost sensors was tested. A GIS-based weighted overlay summation process for the potential sources of air pollution (factories, quarries, and traffic), taking into account the influence of altitude and climate, was used to obtain an air pollution hazard map for Nablus, Palestine. To test the methodology, eight locally calibrated PM sensors (AirUs) were deployed to measure PM<sub>2.5</sub> concentrations for 55 days from 7 January to 2 March 2022. The results of the hazard map showed that 82% of Nablus is exposed to a high and medium risk of PM pollution. Sensors' readings showed a good match between the hazard intensity and PM concentrations. It also shows an elevated PM<sub>2.5</sub> concentrations above WHO guidelines in all areas. In summary, the overall average for PM<sub>2.5</sub> in the Nablus was 48 µg/m<sup>3</sup>. This may indicate the effectiveness of mapping methodology and the use of low-cost, locally calibrated sensors in characterizing air quality status to identify the potential remediation options.



**Citation:** Saleh, T.; Khader, A. Urban Particulate Matter Hazard Mapping and Monitoring Site Selection in Nablus, Palestine. *Atmosphere* **2022**, *13*, 1134. <https://doi.org/10.3390/atmos13071134>

Academic Editors: Patricia Quinn and Chang Hoon Jung

Received: 8 May 2022

Accepted: 15 July 2022

Published: 18 July 2022

**Publisher's Note:** MDPI stays neutral with regard to jurisdictional claims in published maps and institutional affiliations.



**Copyright:** © 2022 by the authors. Licensee MDPI, Basel, Switzerland. This article is an open access article distributed under the terms and conditions of the Creative Commons Attribution (CC BY) license (<https://creativecommons.org/licenses/by/4.0/>).

**Keywords:** particulate matter; low-cost sensors; hazard mapping; GIS; Palestine

## 1. Introduction

Ambient air pollution is a serious problem for many countries around the world. The increase in population and thus the increase in human and industrial activities, have caused noticeable increases in pollutant emissions, which led to many health, economic, and social problems [1]. Air pollution can be defined as the entry of foreign substances into the atmosphere. These materials may include gases, particles, biological materials, or any substances that may harm the health or well-being of living organisms, or cause spoilage or damage to materials [2,3]. Particulate Matter (PM), which is a criteria pollutant [4], is a complex mixture of small particles and liquid droplets, which may include elemental carbon, organic chemicals, metals, acids (such as nitrates and sulfates), and soil and dust particles [5]. PM is divided according to their aerodynamic diameter into PM<sub>10</sub>, which has an aerodynamic diameter of less than 10 µm, and PM<sub>2.5</sub>, which has an aerodynamic diameter of less than 2.5 µm [6].

Numerous epidemiological studies have proven that acute or chronic exposure to air pollutants is associated with many respiratory and cardiovascular diseases, nervous and reproductive system, dysfunction, and cancer [7–11]. Additionally, the effect of exposure to air pollution on cognition and social welfare is noticeable [12]. Several studies around the world have obtained evidence that chronic exposure to air pollution, especially PM<sub>2.5</sub> and NO<sub>2</sub>, increases the spread and lethality of the recent coronavirus (COVID-19). Air pollution affects the body's immunity, making people more vulnerable to pathogens [13,14].

The use of low-cost sensors has increased due to the high cost of reference devices and the difficulty in handling them on site. AirU is a low-cost easy-to-use sensor that can measure PM<sub>10</sub> and PM<sub>2.5</sub> concentrations. It can provide high-precision spatial measurements. The use of low-cost devices should be associated with field calibration to ensure reliable results, and calibration is performed using reference devices [15–17].

In Palestine, the main sources of anthropogenic air pollution are quarries, factories, and traffic. Palestine is notably affected by seasonal dust storms, which are considered a source of biogenic air pollution. There are no Palestinian standards for air quality. A few studies concerning air pollution have been performed, all of which have proven that the concentrations of pollutants exceed the guidelines of the WHO [18,19]. These studies did not take into account the spatial change, the effect of altitude, and the seasonal dust storms; moreover, no clear methodology was used in selecting sampling sites. Random sites selection is not necessarily representative [20]. Site selection process must combine multi-criteria, such as meteorology, pollution sources, and types of pollution sources in terms of impact on human health.

Remote sensing-based aerosol optical depth (AOD) measurements provide a powerful tool for predicting PM concentrations at the regional and global level, for example, NASA provides AOD maps and data with a cell size of 1 km. Previous studies have generally shown a moderate predictive power on a local scale [21,22]. Some interesting studies have provided improved algorithms that combined AOD data with local pollution sources on a 1 km scale using chemistry transport model (CTM) [23–25], which incorporates boundary layer height and air humidity data along with emissions data and patterns. CTM is a powerful method for predicting PM concentrations in monitoring stations, but it is difficult to implement in developing countries due to the large amount of information it requires, such as type of emissions and emission list data and patterns. Obtaining this information requires a lot of effort, time, and money. The use of multi-source big data (indicating that data usually comes from different sources and has different data structures) is often heterogeneous because it is related to dynamic, temporal, and spatial change. In order to overcome this, in recent years, air quality monitoring models that take into account temporal and spatial changes have been introduced. These models require a lot of continuous evidence, such as the readings of air quality monitoring stations, weather stations, etc., so it is difficult to apply these models in developing countries that lack these types of data [26].

Geographic information systems (GIS) have been effectively used as a powerful spatial analysis method that allows the manipulation of different spatial data together with expert opinion in order to make judgments. GIS is an effective tool that is widely used in hazard and site suitability mapping in all areas. It allows the quick and easy visualization of study areas. Providing good spatial representation, the maps are a powerful and clear tool for presenting complex results in a simplified manner thus bridging the gap between experts and users. The GIS-based rasterization is an effective set of tools that can, in general, be applied to any process by which vector information can be converted into a raster format. GIS also supports the weighted overlay summation process that overlays several rasters, using a common measurement scale and weights each according to its importance [27–30]. An interesting study used GIS to apply a suitability analysis approach to establish air quality monitoring stations, the suitability analysis model can be an effective tool for improving existing air quality monitoring networks and drawing the optimum routes for future expansions in monitoring air quality within urban areas [31].

This research aims to develop air pollution hazard mapping methodology and a selection criterion for low-cost air quality sensors' locations and to apply this methodology to the case of Nablus, Palestine. The study area (Figure 1) includes the city of Nablus in addition to the surrounding communities of Beit Wazan, Deir Sharaf, Beit Iba, and Zawata. In this research, these residential communities will be called Nablus. Nablus is located north of the West Bank. The population in 2017 was 163,813 [32]. Topographically, it is a valley between two mountains, with an altitude of about 220–915 m above mean sea

level (AMSL). The climate of the area is Mediterranean climate, which is hot and dry in summer and mild and rainy in winter. Most of the land use is residential, commercial, and industrial, with only 3% green area, according to the Nablus Municipality [30].

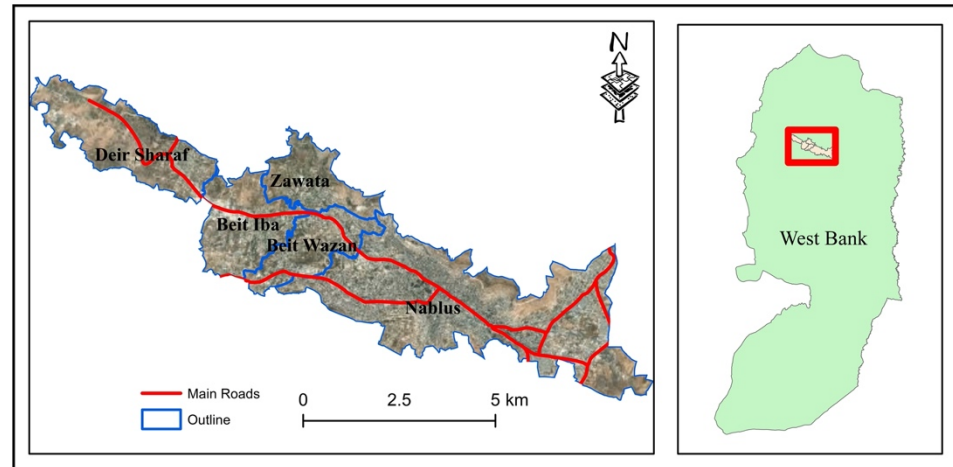


**Figure 1.** Location of the study area.

The topography of the study area, combined with multiple sources of air pollution creates a potential air quality problem that might affect the human health. The main sources of anthropogenic air pollution in the city of Nablus are quarries, factories, and traffic. The area is notably affected by seasonal dust storms, which are considered a source of biogenic air pollution [2]. The factor affecting these criteria is the metrology that controls the dispersion of particles in the atmosphere as a factor of distance from the source of pollution. Each criterion was weighted based on expert decision. After that, GIS was used for the weighted summation process. Finally, based on the produced map the PM concentration was measured in different areas using AirU sensors.

The key output of this research is a site suitability map for low-cost air quality sensors, this map aims to identify the most polluted areas and the most influential source of pollution. This will assist decision-makers in Palestine in setting standards for pollutant concentrations and taking real actions to reduce the risk of air pollution.

## 2. Methodology

The methodology of this research starts with defining the criteria and assigning weights to each criterion. After GIS modeling is used to create raster maps for the study area representing the spatial relation to the possible emission sources, altitude, and wind speed and direction. These maps then are overlaid to create the hazard intensity map for the study area. Finally, the monitoring locations are selected based on the hazard intensity.

The potential local anthropogenic sources of PM in Nablus are quarries, industries, and traffic. The factors that affect these criteria are wind speed, direction, and altitudes [2]. Quarries spatial distribution information was obtained from the portal of spatial information in Palestine GeoMOLG [33]. Figure 2a shows the distribution of 7 quarries and stone crushers in Nablus, which are concentrated in the northwestern part of the city.

A list of all industries was obtained from the Nablus Municipality. The list was revised, and the industries were classified from 1 to 3 based on the industry's potential expected PM emissions. For example, a stone cutting industry was given 3, a sweets bakery was given 2, and a laundry was given 1. The industries with the color-coded classification are shown in Figure 2b. There is an Israeli industrial area near the study area, called the "Kedumim" settlement (Figure 2b). According to [34], this settlement includes a large number of industries, such as paper, cleaning materials, iron, plastic pipes, and others. Therefore, the entire area is considered as an industry with a classification of 3.

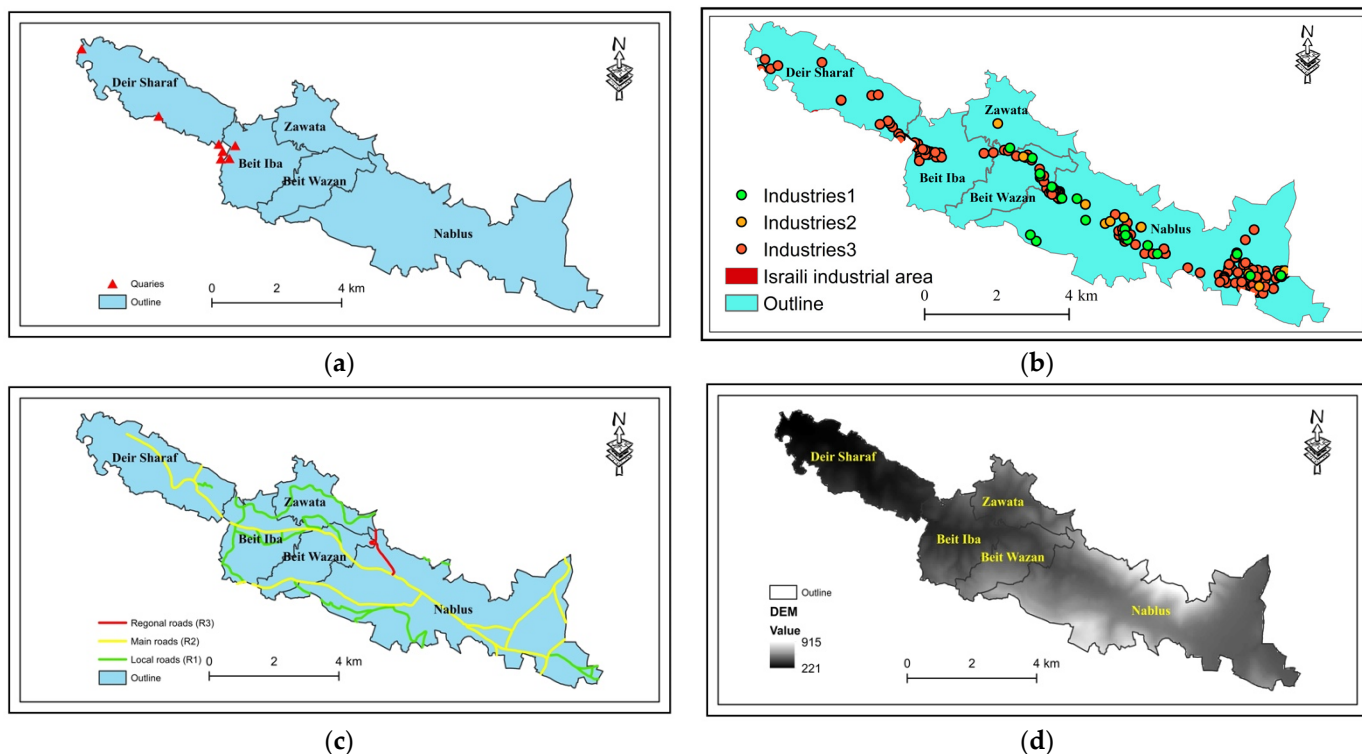


**Figure 2.** Location of potential PM emission sources in the study area: (a) quarries; (b) industries; (c) roads; and (d) topography of the study area.

In order to represent the traffic, the road network data from GeoMOLG was used. This file divides the streets into local, main, and regional, which are classified from 1–3, respectively, according to traffic volumes, as shown in Figure 2c.

The altitude data were obtained from the digital elevation model DEM available at GeoMOLG, as shown in Figure 2d. Wind direction and speed data were obtained online from the Meteoblue website [35], which provides the wind rose at 569 m AMSL at the point 32.22 N 35.25 E in Nablus, as shown in Figure 3.

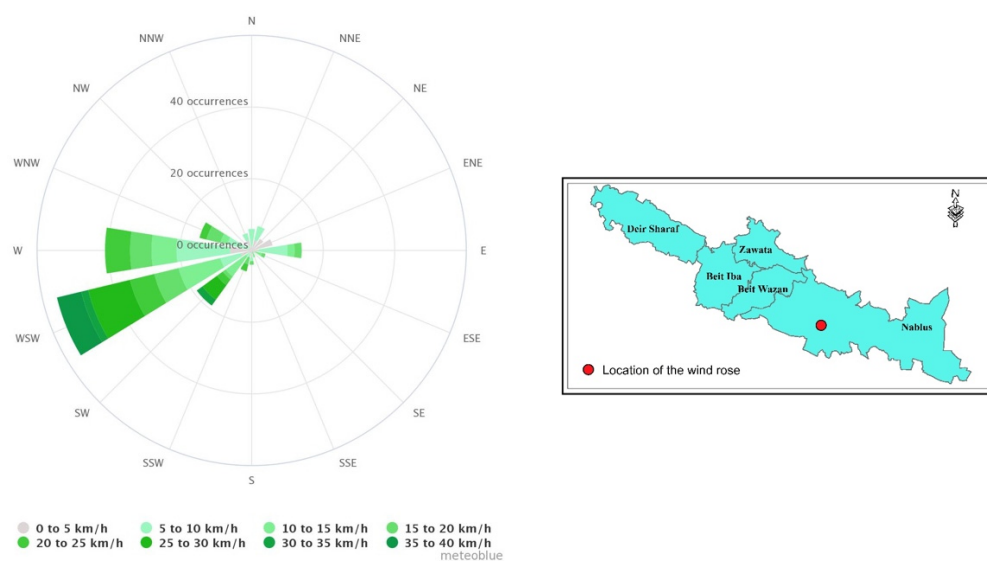


**Figure 3.** Wind rose of Nablus (Meteoblue).

After defining, the four criteria layers were weighted based on their priorities. The industries and quarries were given the highest priority, followed by roads and altitude in

a subjective order. The sub-criteria were divided equally for the industries and roads, as shown in Table 1.

**Table 1.** Criteria and sub-criteria weights.

Criteria	Weight %	Sub-Criteria *	Influence % #
Industry	30%	I1	17
		I2	33
		I3	50
Roads	20%	R1	17
		R2	33
		R3	50
Queries	30%	Q	100
Altitude	20%	A	100

\* I 1, 2, 3: Industries classification based on the potential expected PM emissions; R 1, 2, 3: local, main, and regional roads; Q: Quarries; A: Altitudes; # Influence %: The influence of the raster compared to the other criteria as a percent of 100. Values are rounded down to the nearest integer.

The GIS model shown in Figure 4 was used to overlay the criteria and the weights to create the hazard map. For each criterion (quarries, factories, and roads) the Euclidian distance tool was used to calculate for each cell, the Euclidean distance to the closest source. Then the distance rasters were reclassified into 4 classes at 200, 500, 1000, and 2000 m, which creates the raster distance classification. In parallel, the Euclidian direction tool was used to calculate, for each cell, the direction in degrees to the nearest source. Finally, the weighted overlay tool was used to overlay the two rasters with the same percent of influence for the direction and distance and a scale value of 1 for all the direction values. The DEM rasters were reclassified based on natural breaks (a clustering method designed to determine the best arrangement of values into different classes) into 4 classes; the method seeks to reduce the variance within classes and maximize the variance between classes.

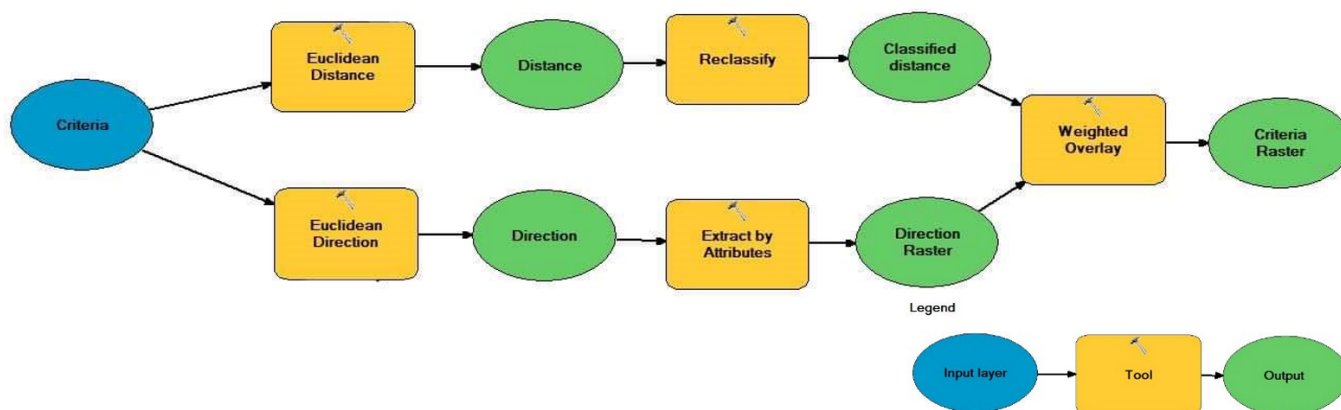


**Figure 4.** GIS model performed on each criterion.

For all the criteria, the resulting rasters were reclassified into 4 classes, the fourth class indicates the nearest place to the source of pollution in the effective wind direction, and so on. These classes are the hazard intensity.

### 3. Results and Discussion

The GIS weighted overlay summation tool was used to calculate the air pollution hazard intensity, this tool overlaid criteria rasters based on their weights, resulting in the hazard intensity map shown in Figure 5. The map shows that 82% of the study area has a high and medium high hazard of PM pollution (hazard indices 3 and 4), while the rest of the area has medium low to low hazard (hazard indices 1 and 2).



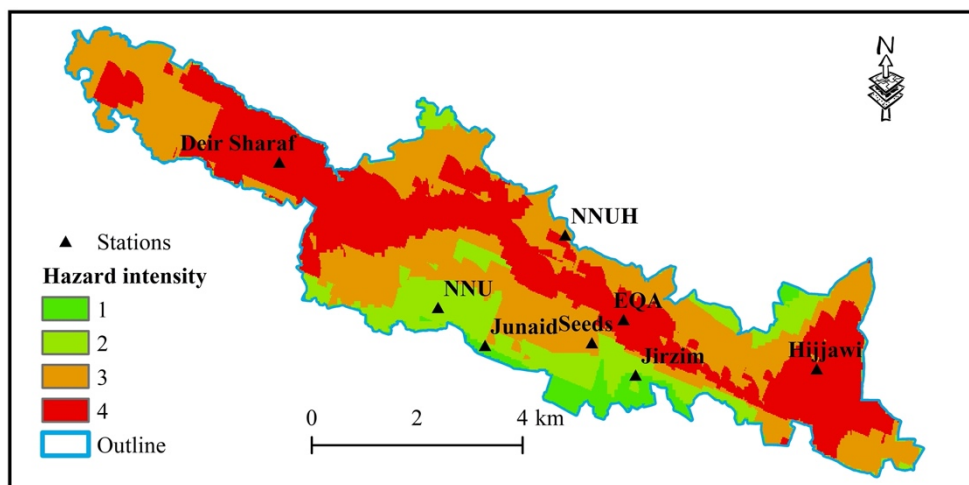


**Figure 5.** Hazard intensity map and locations of monitoring.

Based on the hazard intensity map, eight measuring locations were selected. The locations were distributed to cover the geography of the study area as much as possible, as shown in Figure 5.

In the selected locations, eight low-cost monitoring devices (AirUs) that utilize Plan-tower Particulate Matter Sensor (PMS) 3003 sensors were deployed. The AirUs were developed by the University of Utah’s College of Engineering. The AirUs were calibrated for local PM using a Mini-Vol configured for PM<sub>2.5</sub> collection. For more details about the calibration process, please refer to [2]. The sensors were operated for 55 days from 7 January to 2 March 2022. The location of the device was chosen within the measurement site in a safe place not exposed to rain but exposed to the ambient air. Figure 6 shows the daily averages (the AirUs were programmed for one-minute averages) of the PM<sub>2.5</sub> concentrations from each of the eight sites. As shown in the figure, the PM concentrations were found to be highly variable and exceeded WHO guidelines most of the time. Table 2 shows the average, maximum, and minimum PM concentrations (in µg/m<sup>3</sup>) in the eight sampling locations. Unfortunately, the sensor measurements in NNUH only lasted for 26 days due to vandalism.

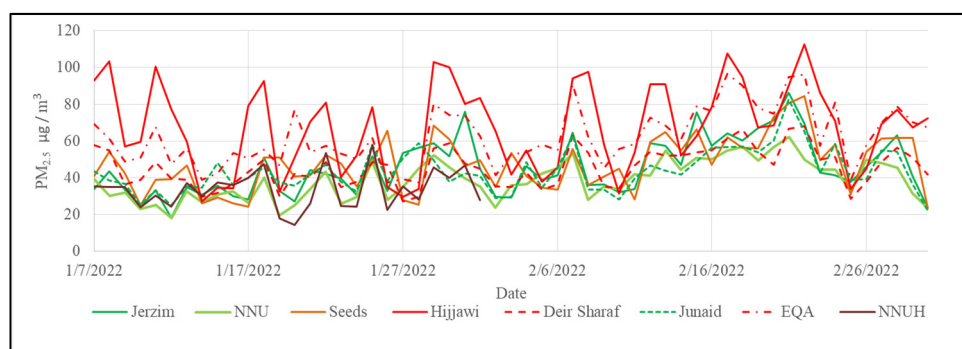


**Figure 6.** Average daily PM<sub>2.5</sub> concentration in each measuring site.

The measuring results shows that the average daily PM<sub>2.5</sub> concentrations exceeded the WHO guidelines (10 µg/m<sup>3</sup> 24 h) 73% to 100% of the time in all locations. The overall average PM<sub>2.5</sub> concentration in the eight locations was calculated to be 48 µg/m<sup>3</sup>. Figure 7 shows the correlation between the average PM<sub>2.5</sub> (in µg/m<sup>3</sup>) and the hazard intensity values. This correlation shows that PM<sub>2.5</sub> concentrations are commensurate with the hazard intensity that was proposed through the air pollution hazard map. However, the average PM<sub>2.5</sub> concentrations in Jerzim and Junaid locations (hazard intensity 1) were not

the lowest, although they had the lowest hazard intensity. After investigating, it appeared that local sources of air pollution affected the measurements (hookah smokers in the case of Jerzim site and construction work near the Junaid site). This observation suggest that more sensors are needed to overcome the inherent uncertainty in PM<sub>2.5</sub> emissions.

**Table 2.** Average, maximum, and minimum PM<sub>2.5</sub> values (in µg/m<sup>3</sup>) in the eight sampling locations.

Location	Hazard Intensity	Average ± 95% CL	n/N *	Max. Value	Date	Min. Value	Date
Jerzim	1	45.36 ± 4.13	52/55	86.37	21 February	18.18	12 January
Junaid	1	43.60 ± 3.13	54/55	82.53	21 February	22.36	2 March
NNU	2	38.76 ± 2.93	50/55	62.32	21 February	18.26	12 January
Seeds	3	47.58 ± 3.98	51/55	84.61	22 February	23.78	2 March
NNUH	3	33.78 ± 4.30	19/26	57.94	25 January	14.52	20 January
Hijjawi	4	67.43 ± 6.46	55/55	112.48	22 February	27.35	14 January
EQA	4	62.37 ± 4.25	55/55	96.41	17 February	37.47	28 January
Deir Sharaf	4	45.70 ± 2.85	55/55	68.25	22 February	27.22	27 January

\* n is the numbers of days in which the 24 h WHO guideline was exceeded, and N is the number of sampling days.

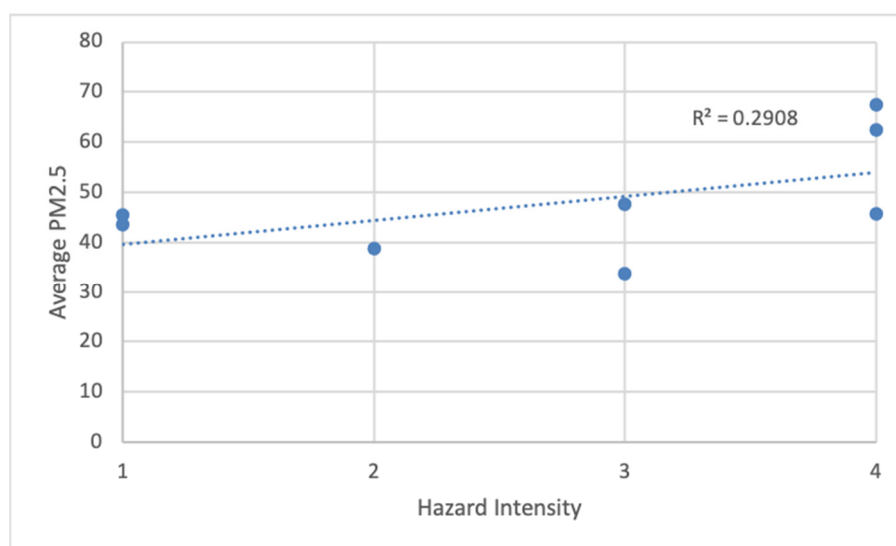


**Figure 7.** Correlation between average PM<sub>2.5</sub> (in µg/m<sup>3</sup>) and hazard intensity.

#### 4. Conclusions

In this study a GIS based weighted overlay summation process was used to develop an air pollution hazard map for Nablus by weighing the criteria of potential air pollution sources (factories, quarries, and traffic), with weights of 30%, 30%, and 20%, respectively, against a weight of 20% for altitude, taking into account the wind speed and direction. The results of the risk map showed that 82% of Nablus is exposed to a high and medium risk of particulate air pollution. Based on the hazard intensity, eight low-cost AirU sensors were deployed in different locations and measured PM<sub>2.5</sub> concentrations for 55 days. The results showed a good match between the hazard intensity and PM concentrations, and the PM<sub>2.5</sub> 24 h concentrations were elevated above WHO guidelines in all areas. In summary, the overall average for PM<sub>2.5</sub> in the Nablus region was 48 µg/m<sup>3</sup>. The matching between the PM concentrations and the hazard map and the closeness of the concentrations to the concentrations (as shown by [2,18]), which gives an impression of the effectiveness of the mapping methodology and the use of low-cost sensors in characterizing the PM situation in urban areas. This helps decision makers to take appropriate decisions. Further

studies could be conducted using a denser sensor network to determine more area-specific pollutant levels, local source strengths, and the impact of seasonal dust storms. It should be noted that the outcomes of the study could have been significantly improved if there was a comprehensive database of the potential pollution sources, and an adequate network of monitoring stations with historical records.

**Author Contributions:** Conceptualization, T.S. and A.K.; methodology, T.S. and A.K.; software, T.S. and A.K.; validation, T.S. and A.K.; formal analysis T.S. and A.K.; writing—original draft preparation, T.S. and A.K.; writing—review and editing, T.S. and A.K.; visualization, T.S.; supervision, A.K. All authors have read and agreed to the published version of the manuscript.

**Funding:** This research received no external funding.

**Institutional Review Board Statement:** Not applicable.

**Informed Consent Statement:** Not applicable.

**Data Availability Statement:** Data is available upon request.

**Acknowledgments:** The Authors are thankful to the Nablus Municipality and the Environmental Quality Authority/Nablus for providing data on factories in the study area.

**Conflicts of Interest:** The authors declare no conflict of interest.

## References

1. Manisalidis, I.; Stavropoulou, E.; Stavropoulos, A.; Bezirtzoglou, E. Environmental and Health Impacts of Air Pollution: A Review. *Front. Public Health* **2020**, *8*, 14. [CrossRef] [PubMed]
2. Khader, A.; Martin, R.S. Use of low-cost ambient particulate sensors in Nablus, Palestine with application to the assessment of regional dust storms. *Atmosphere* **2019**, *10*, 539. [CrossRef]
3. Mayer, H. Mayer: Cities. *Atmos. Environ.* **1999**, *33*, 4029–4037. [CrossRef]
4. Criteria Air Pollutants. Available online: <https://www.epa.gov/criteria-air-pollutants#self> (accessed on 10 December 2021).
5. Cascio, W.E.; Gilmour, M.I.; Peden, D.B. Ambient air pollution and increases in blood pressure: Role for Biological Constituents of Particulate Matter. *Hypertension* **2015**, *66*, 469–472. [CrossRef] [PubMed]
6. Davidson, C.I.; Phalen, R.F.; Solomon, P.A. Airborne particulate matter and human health: A review. *Aerosol Sci. Technol.* **2005**, *39*, 737–749. [CrossRef]
7. Brook, R.D. You are what you breathe: Evidence linking air pollution and blood pressure. *Curr. Hypertens. Rep.* **2005**, *7*, 427–434. [CrossRef]
8. Nowak, D.J.; Hirabayashi, S.; Doyle, M.; McGovern, M.; Pasher, J. Air pollution removal by urban forests in Canada and its effect on air quality and human health. *Urban For. Urban Green.* **2018**, *29*, 40–48. [CrossRef]
9. Rajak, R.; Chattopadhyay, A. Short and Long Term Exposure to Ambient Air Pollution and Impact on Health in India: A Systematic Review. *Int. J. Environ. Health Res.* **2020**, *30*, 593–617. [CrossRef]
10. Sacks, J.D.; Fann, N.; Gumy, S.; Kim, I.; Ruggeri, G.; Mudu, P. Quantifying the public health benefits of reducing air pollution: Critically assessing the features and capabilities of WHO's AirQ+ and U.S. EPA's environmental benefits mapping and analysis program-community edition (BenMAP-CE). *Atmosphere* **2020**, *11*, 516. [CrossRef]
11. World Health Organization. *Quantification of the Health Effects of Exposure to Air Pollution Report of a WHO Working Group*; WHO: Bilthoven, The Netherlands, 2000; p. 34.
12. Zhang, X.; Chen, X.; Zhang, X. The impact of exposure to air pollution on cognitive performance. *Proc. Natl. Acad. Sci. USA* **2018**, *115*, 9193–9197. [CrossRef]
13. Copat, C.; Cristaldi, A.; Fiore, M.; Grasso, A.; Zuccarello, P.; Signorelli, S.S.; Conti, G.O.; Ferrante, M. The role of air pollution (PM and NO<sub>2</sub>) in COVID-19 spread and lethality: A systematic review. *Environ. Res.* **2020**, *191*, 110129. [CrossRef] [PubMed]
14. Yao, Y.; Pan, J.; Liu, Z.; Meng, X.; Wang, W.; Kan, H.; Wang, W. Temporal association between particulate matter pollution and case fatality rate of COVID-19 in Wuhan. *Environ. Res.* **2020**, *189*, 109941. [CrossRef] [PubMed]
15. Castell, N.; Dauge, F.R.; Schneider, P.; Vogt, M.; Lerner, U.; Fishbain, B.; Broday, D.; Bartonova, A. Can commercial low-cost sensor platforms contribute to air quality monitoring and exposure estimates? *Environ. Int.* **2017**, *99*, 293–302. [CrossRef] [PubMed]
16. Miskell, G.; Salmond, J.; Williams, D.E. Low-cost sensors and crowd-sourced data: Observations of siting impacts on a network of air-quality instruments. *Sci. Total Environ.* **2017**, *575*, 1119–1129. [CrossRef] [PubMed]
17. Thompson, J.E. Crowd-sourced air quality studies: A review of the literature & portable sensors. *Trends Environ. Anal. Chem.* **2016**, *11*, 23–34. [CrossRef]
18. Abdeen, Z.; Qasrawi, R.; Heo, J.; Wu, B.; Shpund, J.; Vanger, A.; Sharf, G.; Moise, T.; Brenner, S.; Nassar, K.; et al. Spatial and temporal variation in fine particulate matter mass and chemical composition: The middle east consortium for aerosol research study. *Sci. World J.* **2014**, *2014*, 878704. [CrossRef]



19. Jodeh, S.; Hasan, A.R.; Amarah, J.; Judeh, F.; Salghi, R.; Lgaz, H.; Jodeh, W. Indoor and outdoor air quality analysis for the city of Nablus of residential homes. *Air Qual. Atmos. Health* **2018**, *11*, 229–237. [[CrossRef](#)]
20. Ott, W.R. Development of criteria for siting air monitoring stations. *J. Air Pollut. Control Assoc.* **1977**, *27*, 543–547. [[CrossRef](#)]
21. Van Donkelaar, A.; Martin, R.V.; Brauer, M.; Kahn, R.; Levy, R.; Verduzco, C. Global Estimates of Ambient Fine Particulate Matter Concentrations from Satellite-Based Aerosol Optical Depth: Development and Application. *Environ. Health Perspect.* **2010**, *118*, 847–855. [[CrossRef](#)]
22. Hu, Z. Spatial analysis of MODIS aerosol optical depth, PM<sub>2.5</sub>, and chronic coronary heart disease. *Int. J. Health Geogr.* **2009**, *8*, 27. [[CrossRef](#)]
23. Chu, Y.; Liu, Y.; Li, X.; Liu, Z.; Lu, H.; Lu, Y.; Mao, Z.; Chen, X.; Li, N.; Ren, M.; et al. A review on predicting ground PM<sub>2.5</sub> concentration using satellite aerosol optical depth. *Atmosphere* **2016**, *7*, 129. [[CrossRef](#)]
24. Paciorek, C.J.; Liu, Y.; Moreno-Macias, H.; Kondragunta, S. Spatiotemporal associations between GOES aerosol optical depth retrievals and ground-level PM<sub>2.5</sub>. *Environ. Sci. Technol.* **2008**, *42*, 5800–5806. [[CrossRef](#)] [[PubMed](#)]
25. van Donkelaar, A.; Martin, R.V.; Park, R.J. Estimating ground-level PM<sub>2.5</sub> using aerosol optical depth determined from satellite remote sensing. *J. Geophys. Res. Atmos.* **2006**, *111*, 1–10. [[CrossRef](#)]
26. Huang, W.; Li, T.; Liu, J.; Xie, P.; Du, S.; Teng, F. An overview of air quality analysis by big data techniques: Monitoring, forecasting, and traceability. *Inf. Fusion* **2021**, *75*, 28–40. [[CrossRef](#)]
27. Nadal, M.; Cadiach, O.; Kuma, V.; Poblet, P.; Mari, M.; Schuhmacher, M.; Domingo, J.L. Health risk map of a petrochemical complex through gis-fuzzy integration of air pollution monitoring data. *Hum. Ecol. Risk Assess.* **2011**, *17*, 873–891. [[CrossRef](#)]
28. Lahr, J.; Kooistra, L. Environmental risk mapping of pollutants: State of the art and communication aspects. *Sci. Total Environ.* **2010**, *408*, 3899–3907. [[CrossRef](#)] [[PubMed](#)]
29. Anh, N.K.; Phonekeo, V.; My, V.C.; Duong, N.D.; Dat, P.T. Environmental hazard mapping using GIS and AHP-A case study of Dong Trieu District in Quang Ninh Province, Vietnam. *IOP Conf. Ser. Earth Environ. Sci.* **2014**, *18*, 012045. [[CrossRef](#)]
30. Chung, C.J.; Hsieh, Y.Y.; Lin, H.C. Fuzzy inference system for modeling the environmental risk map of air pollutants in Taiwan. *J. Environ. Manag.* **2019**, *246*, 808–820. [[CrossRef](#)]
31. Alsahli, M.M.; Al-Harbi, M. Allocating optimum sites for air quality monitoring stations using GIS suitability analysis. *Urban Clim.* **2018**, *24*, 875–886. [[CrossRef](#)]
32. PCBS. *Preliminary Results of the Population, Housing and Establishments Census 2017*; Palestinian Central Bureau of Statistics: Ramallah, Palestine, 2018; p. 82.
33. GeoMOLG Palestinian Ministry of Local Government. Available online: [geomolg.ps](http://geomolg.ps) (accessed on 25 December 2021).
34. Vanguard, T.; Resettlement, J. *KEDUMIM Zionism Is Still Alive in Kedumim*; Kedumim: Kedumim, Israel, 2020.
35. Meteoblue Weather Nablus—Meteoblue. Available online: [https://www.meteoblue.com/en/weather/week/nablus-palestine\\_282615](https://www.meteoblue.com/en/weather/week/nablus-palestine_282615) (accessed on 16 March 2021).